

Radiated Electromagnetic Interference(Emi) Mechanism of High Power Inverter

Qiangqiang Liu

Received: 14 December 2018 Accepted: 31 December 2018 Published: 15 January 2019

Abstract

In this paper, the generation mechanism of radiated EMI noise in inverter circuit is analyzed. On the basis of analyzing the equivalent model of common mode and differential mode radiated EMI noise, the radiated EMI noise is separated by common mode and differential mode by using the fast Fourier transform principle. The effectiveness of the radiated EMI noise separation method is verified by experiments.

Index terms— high-power inverter, electromagnetic interference(emi), radiation emission (re), common mode radiation,

with the rapid development of power electronics, inverter systems with highpower inverter power supply as the core are more and more widely used in large-scale power equipment [1][2][3][4][5]. However, the increase of power density leads to the increasingly complex electromagnetic environment inside the inverter system [6][7][8][9][10]. The resulting radiated electromagnetic interference can cause equipment failure and pose a potential hazard to the safe and reliable operation of itself and other surrounding equipment [11][12]. Therefore, it is necessary to study the mechanism of radiated electromagnetic interference of high-power inverters [13].

The radiated EMI noise is generated by the inverter circuit and the loop equivalent antenna [14][15]. The device under tested (EUT) is placed at the coordinates (x, y, z) , the measured point is at (x', y', z') , and the length of the EUT equivalent radiating antenna is l , then the equivalent radiated antenna is measured. The distance between points can be expressed as R . Where R is the distance between the origin and the point to be measured, and n is the unit vector in the R direction. The wavelength corresponding to the radiation noise is

In the above formula, c is 3×10^8 m/s, λ is the wavelength corresponding to the radiation noise, and f is the frequency of the radiated EMI noise caused by the EUT.

Because the size of the high-power inverter power cabinet is $800\text{mm} \times 500\text{mm} \times 1500\text{mm}$ (width \times depth \times height), and according to the simulation calculation f is about 80kHz, λ is 3750m, the transmission control cabinet The size is obviously less than 1/10 of the wavelength of the radiation. It can be considered that the above radiation test condition is a small size characteristic, and the current density in the equivalent antenna is J , which can be derived.

A is a retarded potential, and k is the wave vector. The term in the denominator of (3) can be omitted, and will be expanded by

The first two parts of equation (4) represent electric dipole common mode radiation and magnetic dipole differential mode radiation, respectively.

1 II.

2 Radiated EMI Noise Modeling a) Common mode EMI noise model

As shown in Fig. 1, for common mode radiation, it can be equivalent to an electric dipole antenna, and the delay potential is the first part of equation (4). $c = f \lambda$ (2)

Author Jiangsu Institute of Metrology, Nanjing Jiangsu China. e-mail: 448221017@qq.com Author ? ? ? ¥ §: Nanjing Normal University, Nanjing, Jiangsu. China. e-mail: 1730312514@qq.com () 0 (4 jk R n x J x e A(x)=

44 $dV R n x ? ? ? ? ? ? ? ? ? ? (3) n x ? ? ? j k n x e ? ? ? k n x ? ? . 0 () (1) 4 j k R e A(x) = J x j k n x dV ?$
 45 $? ? ? ? ? ? ? ? ? ? (4) 0 () () 4 j k e R e A x J x dV R ? ? ? ? ? ? ? (5)$
 46 Global Journal of Researches in Engineering () Volume XIX Issue III Version I

3 Introduction : ?

47 In the electric dipole antenna, there are n_i particles with a velocity of v_i and a charge of q_i per unit volume. then
 48 Where is the first derivative of the electric dipole moment versus time.

49 Therefore, the magnetic field strength, electric field strength, energy flow density and radiation power of the
 50 electric dipole can be derived.

51 According to equation (??) and Maxwell's equations, the calculated common mode radiated noise generated
 52 by the electric dipole at far field r is I_{CM} is the common mode current in the electric dipole, l is the length
 53 of the electric dipole antenna, and r is the distance between the measured point and the center of the electric
 54 dipole. Therefore, equations (??), (9), and (1) can describe the principle and model of electric dipole common
 55 mode radiation noise.
 56

4 b) Differential mode EMI noise model

57 As shown in Fig. 2, for differential mode radiation, it can be equivalent to a magnetic dipole antenna, which
 58 delays the second part of the potential size formula (4).
 59

5 Fig. 2: Differential mode noise model

60 The magnetic field strength, electric field strength, energy flow density and radiant power of the magnetic dipole
 61 antenna are From the equation (11) and the Maxwell equations, considering the grounding total reflection, the
 62 differential mode radiated noise of the magnetic dipole antenna at the far field r I_{DM} is the differential mode
 63 current in the magnetic dipole, A is the area of the magnetic dipole antenna, and r is the distance between the
 64 measured point and the center of the electric dipole. Therefore, equations (11), (12), and Fig. 2 can describe the
 65 principle and model of magnetic dipole differential mode radiated noise.
 66

6 III. Radiated EMI Noise Separation Method

67 The second section of the above section establishes the electric dipole common mode radiation and the magnetic
 68 dipole differential mode radiation acoustic model, The nature of the radiated noise is analyzed when the radiated
 69 noise is suppressed. Therefore, this section designs a radiated noise separation method based on short-time
 70 fast Fourier transform and independent component analysis for common mode noise and differential mode noise
 71 electromagnetic characteristics. $i i i i J n q v ? ? (6) i i P = q v ? (7) CM CM f l i E r ? ? ? (9) 0 () () 4 j k R j k e$
 72 $A x = J x n x dV R ? ? ? ? ? ? ? ? (10) 0 2 () 4 j k R DM e B A = m n n c R ? ? ? ? ? ? ? 0 () 4 j k R DM e E$
 73 $c B A m n c R ? ? ? ? ? ? ? 2 4 0 2 2 3 2 \sin 32 DM m S c R ? ? ? ? ? ? n 2 4 0 3 12 DM m P c ? ? ? (11) 2 14$
 74 $2.632 10 DM DM f A I E r ? ? ? (12)$
 75

76 Using the field probe to receive the radiated noise $Z_1(t), Z_2(t), \dots, Z_N(t)$ of the N sets of EUTs, perform short-time
 77 fast Fourier transform on the acquired time domain signal $Z(t)$. Where $\omega(t)$ is the time window and $*$ indicates
 78 its conjugate complex number. The time-rate energy distribution (instantaneous power spectral density) of the
 79 STFT is the square of the STFT(t, f) modulus.

80 The digital representation of the STFT can be derived from the equations (??3) and (??4).

81 Where N represents the amount of FFT data, and n and k represent the discrete time number of the time-
 82 frequency and the number of frequency grids, respectively. In the application, the fast algorithm of equation (
 83 16) is generally implemented by Fourier transform.

84 Through independent component analysis, the characteristics of the received noise signal are extracted, and
 85 then the short-time fast Fourier transform is used to convert the separated time domain noise signal into
 86 the frequency domain, and compared with the circuit under test, the source of the radiated electromagnetic
 87 interference noise is located. the specific method implementation steps are as follows: frequency detection range
 88 of 10 kHz to 2 GHz as shown in Fig. ???. The multi track high-speed oscilloscope uses the Tektronix DPO5204
 89 model with a bandwidth of up to 2 GHz and four test channels with a sampling rate range of 5 GS/s -10 GS/s. In
 90 the experiment, the sampling rate of the oscilloscope DPO5204 is set to 1GS/s, and the EUT radiated noise time
 91 domain signal can be acquired. Firstly, the radiated noise mixed time domain signal of the high-power inverter
 92 power supply is collected. The measured near-field noise test result is shown in Fig. 6. After the noise signal is
 93 introduced into MATLAB, the time domain characteristics of the noise () | () | SPEC t f STFT t f ? ? ? (14) 1
 94 $1 0 2 () [()] \exp () N i k i STFT n k = x i-n j N ? ? ? ? ? ? ? ? (15) 2 () | () | SPEC n k STFT t f ? ? ? (16)$

7 IV. Radiated EMI Noise Separation Experiment

95 This verification experiment uses a multi track high speed oscilloscope to measure the radiated noise time domain
 96 signal of the EUT through a mufti channel test port with a near-field magnetic field probe, as shown in Fig. ???.
 97

98 The near-field magnetic field probe uses Rhode & Schwarz's near-field probe set HZ-11, which has a signal are
 99 shown in Fig. 6 (a). Perform independent component analysis, as shown in Fig. 6(b). There are two independent

100 noise signals $Z1(t)$ and $Z2(t)$. The timefrequency analysis is shown in Fig. 7. As can be seen from Fig. 7(a), the
101 data with the strongest energy in the noise is extracted as shown in Table 1. The average value of the data in
102 the table is about 240 MHz. It can be seen that the noise is strongest around 240 MHz, and the internal inverse
103 is observed. The variable circuit found that the crystal frequency of the control board is 30MHz, and 240MHz
104 is its frequency multiplication, so the noise is the radiation noise generated by the 30MHz crystal oscillator. As
105 seen in Fig. 7(b), the noise is the strongest at 300KHz, and the noise signal data at the strongest energy is
106 extracted as shown in Table 2. The average value is 299.85KHz, which is compared with the internal inverter
107 circuit. The power master chip operates at a frequency of 100 kHz and 300 kHz as its frequency multiplier.
108 Therefore, the noise after the separation is the radiation noise of the 100 KHz master chip. It can be seen that
109 the radiation noise of the device is mainly generated by the 30M crystal oscillator and the 100KHz main control
110 chip. 1 and 2, the energy intensity of the 30MHz noise signal is stronger in the noise signals after separation
111 between the two groups. Therefore, the 30MHz noise signal is the main cause of the radiation noise exceeding
112 the standard of the device under test. From the above analysis, the 30MHz crystal oscillator is large. The main
113 reason for the excessive radiation noise of the power inverter power supply cabinet provides a theoretical basis
114 for the suppression of subsequent radiation noise.

115 8 Conclusion

116 In short, the mechanism of radiated EMI noise generation in inverter circuit has been analyzed, and the
117 method of common mode and differential mode separation of radiated EMI noise by using the principle of
118 fast Fourier transform is proposed. The effectiveness of the method of radiating EMI noise separation is verified
by experiments. Sex. As a result, a better solution to EMI noise can be proposed. ^{1 2 3}

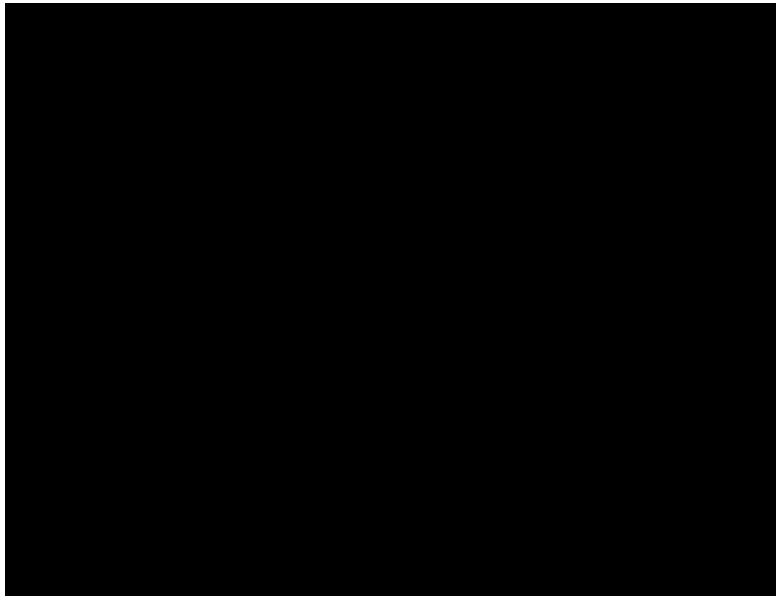


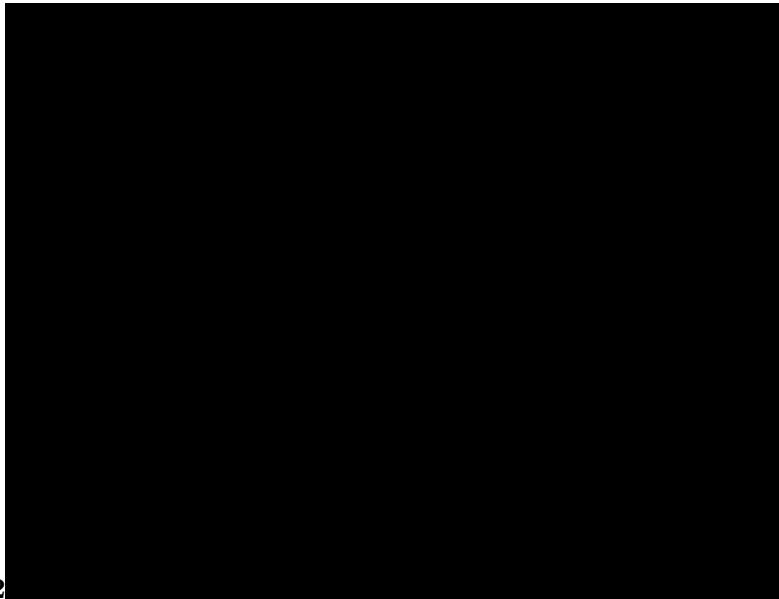
Figure 1: Fig. 1 :

119

¹Year 2019 F © 2019 Global Journals I.

²© 2019 Global Journals

³Radiated Electromagnetic Interference(Emi) Mechanism Of High Power Inverter



2

Figure 2: 2 (

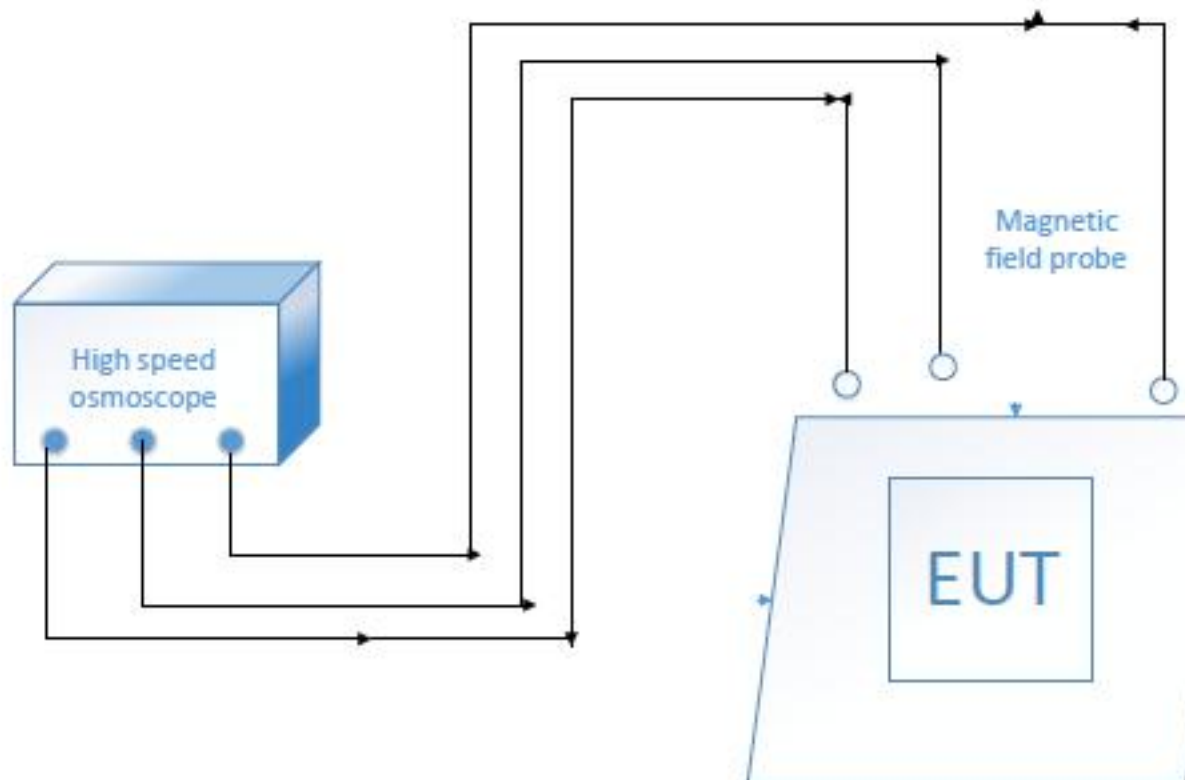
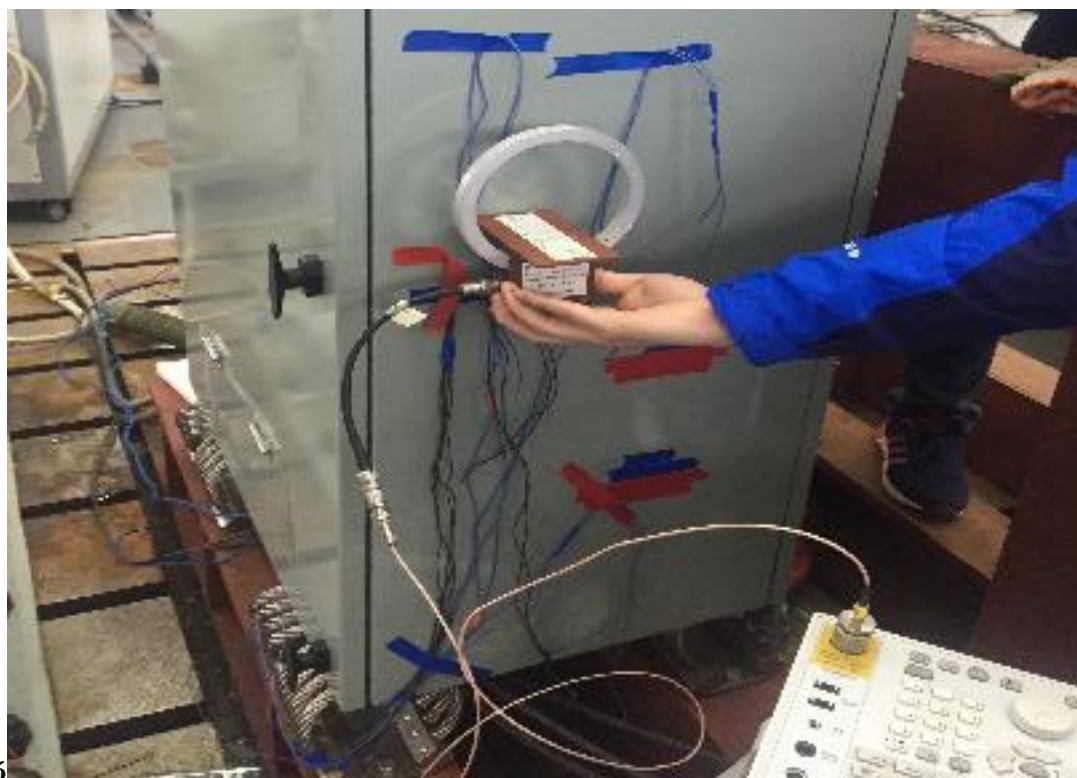


Figure 3:



345

Figure 4: Fig. 3 :Fig. 4 :Fig. 5 :

8 CONCLUSION

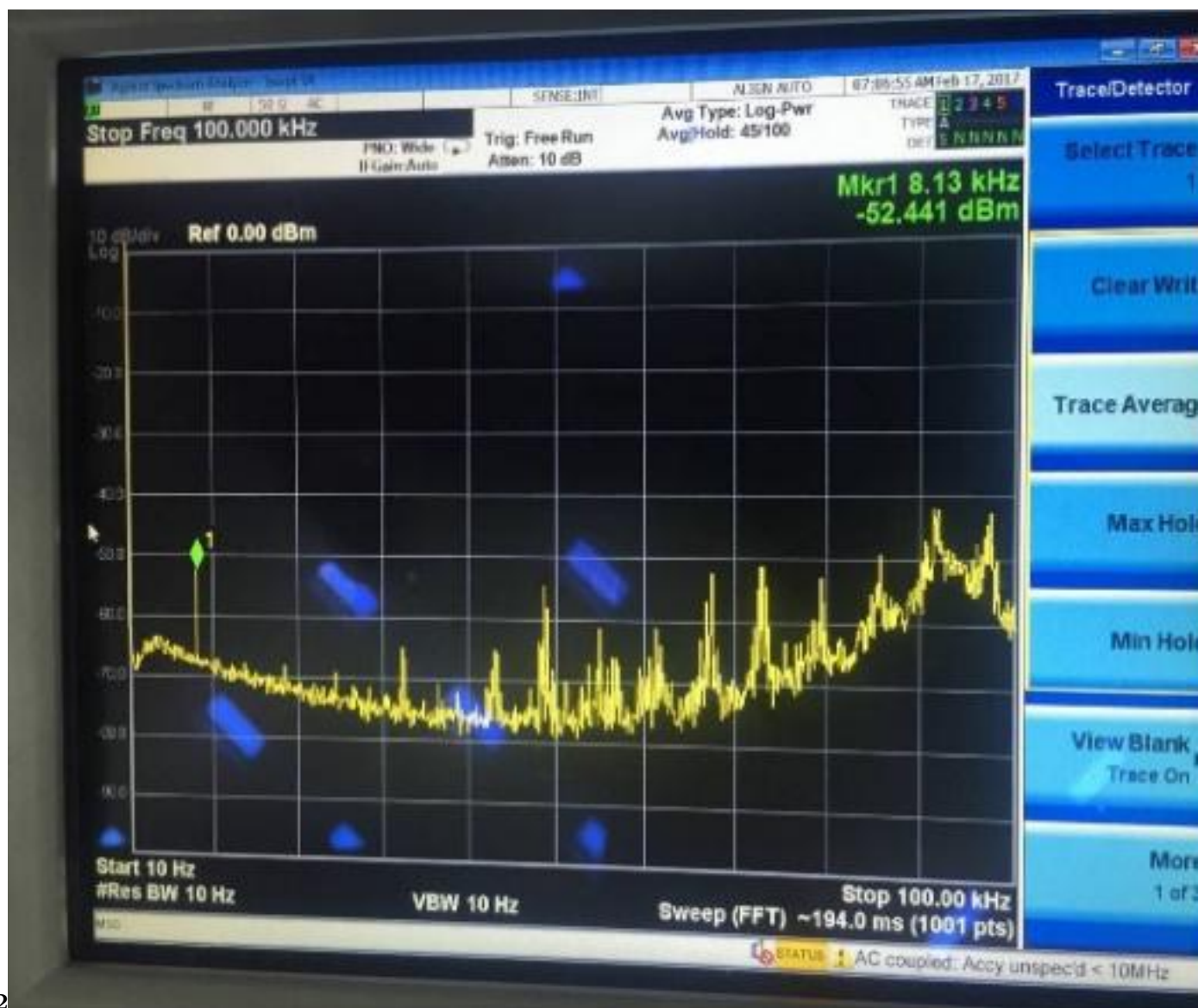
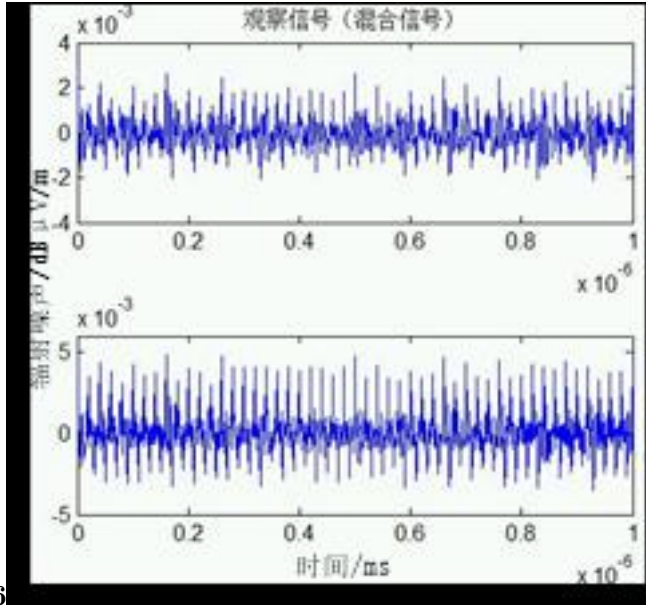
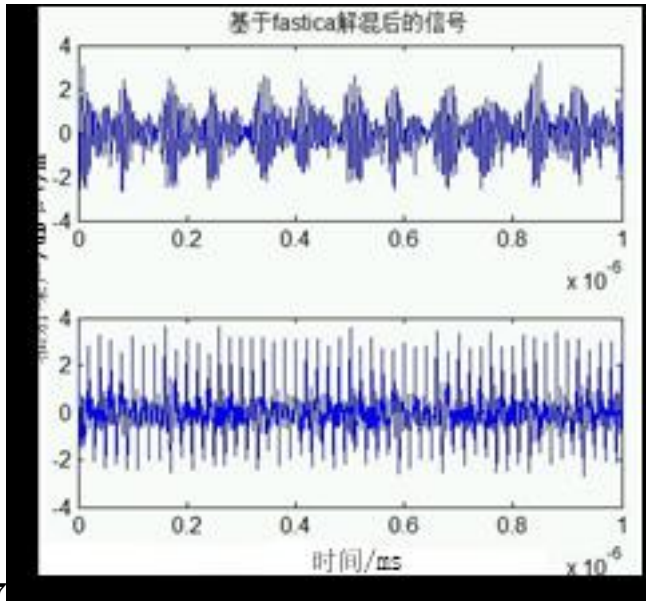


Figure 5: 2



6

Figure 6: Fig. 6 :



7

Figure 7: Fig. 7 :

1

Figure 8: Table 1 :

2

Figure 9: Table 2 :

-
- 120 [He et al. ()] *Analysis of the effect of stray magnetic field on conduction CSEE*, J P He , W Chen , J G Jiang .
121 2005. 25 p. .
- 122 [Qian and Cheng ()] *Electromagnetic Interference Design and Interference Suppression Technology for Power*
123 *Electronic Systems*, Z M Qian , W J Cheng . 2000. Zhejiang University Press. p. .
- 124 [Qian et al. ()] ‘EMC Design of High Power Converters’. G L Qian , Z Y Lu , X N He . *Proceedings of the 14th*
125 *National Conference on Power Technology*, (the 14th National Conference on Power Technology) 2001. p. .
- 126 [Zhang et al. ()] ‘Full-Bridge Circuit Common Mode Suppression Technology Based on Drive Pulse Self-
127 Calibration’. K Zhang , Z Y Liu , X J Qi . *Proceedings of the CSEE*, (the CSEE) 2007. 27 p. .
- 128 [GB T 17626-2006. Electromagnetic Compatibility Test Methods and Testing Techniques ()] *GB T 17626-2006.*
129 *Electromagnetic Compatibility Test Methods and Testing Techniques*, 2006.
- 130 [Yuan and Qian ()] ‘Modeling of Power MOSFETs for Conducting EMI’. Y S Yuan , G L Qian . *Journal of*
131 *Zhejiang University (Engineering Science)* 2003. 37 (2) p. .
- 132 [Sarikhani et al. ()] ‘Optimum Equivalent Models of Multi-source Systems for the Study of Electromagnetic
133 Signatures and Radiated Emissions From Electric Drives’. A Sarikhani , M Barzegaran , O A Mohammed .
134 *IEEE Transactions on Magnetics Mag* 2012. 48 (2) p. .
- 135 [He et al. ()] ‘Research on Common Mode Conducted Interference Model of Switching Power Supply’. J P He ,
136 W Chen , J G Jiang . *Proceedings of the CSEE*, (the CSEE) 2005. 25 p. .
- 137 [Zhou ()] *Research on Common Mode EMI Analysis and Active Suppression Technology for Single-Phase Inverter*,
138 Y B Zhou . 2006. Huazhong University of Science and Technology (factor correction circuit. Proceedings of
139 the)
- 140 [Zhang et al. ()] ‘Research on common mode equivalent circuit of single-phase full-bridge inverter’. K Zhang , H
141 S Fang , Y B Zhou . *Transactions of China Electrotechnical Society* 2007. 22 (2) p. .
- 142 [Peng and Tang ()] ‘Research on Electromagnetic Compatibility of Transmission System’. Y B Peng , Y Q Tang
143 . *Electric Drive*, 2007. 16 p. .
- 144 [Zhang ()] *Research on Electromagnetic Interference and Suppression of Electric Vehicle Motor Inverter System*,
145 X Y Zhang . 2016. Beijing Institute of Technology
- 146 [Su and Li ()] ‘Research on Eliminating Highorder Harmonics of Inverter Output Voltage’. K C Su , J Li . *Journal*
147 *of South China University of Technology(Natural Science Edition)* 1991. 19 (1) p. .
- 148 [Specification and Measurement Methods for Radio Disturbance and Immunity Measurement Equipment ()]
149 *Specification and Measurement Methods for Radio Disturbance and Immunity Measurement Equipment*, GB
150 T 6113-2008. 2008.
- 151 [Hertz ()] *Thermal and EMI Modeling and Analysis of a Boost PFC Circuit Designed Using a Genetic-Based*
152 *Optimization*, E Hertz . 2001. Virginia Tech.